

Supramolecular Medicinal Chemistry: Mixed-Ligand
Coordination Complexes

Zhenbo Ma and Brian Moulton*

Department of Chemistry, Brown University, 324 Brook Street, Providence,
Rhode Island 02912

Received January 18, 2007; Revised Manuscript Received April 9, 2007; Accepted April 12, 2007

Abstract: We report on the supramolecular synthesis and characterization of examples from three series of mixed-ligand coordination complexes composed of copper(II), a drug, and an ancillary ligand (AL). Particularly, we demonstrate how the judicious choice of an ancillary ligand affords a large degree of control over the relative lipophilicity/hydrophilicity of the complex in relation to the uncomplexed drug molecule. Furthermore, we demonstrate several important factors to consider in the design of such complexes such as the additive–constitutive nature of the partition coefficient of the ancillary ligand and the relative size of the two types of ligands.

Keywords: Solubility; lipophilicity; metal–drug; mixed ligand; QSAR; NSAID; partition coefficient; solubility ratio; pharmaceutical cocrystal; complementary; noncovalent

Introduction

Medicinal chemistry involves the design and synthesis of molecules having a therapeutic benefit and is most often associated with the discovery and early development stages of drug's life cycle. Furthermore, the primary focus is generally the derivatization of lead compounds or drug candidates via covalent organic transformations. Despite the rapid evolution of supramolecular synthesis,¹ the concept of *supramolecular medicinal chemistry*² is unfamiliar to most practitioners, with the exception of its inherent application in drug design, such as in molecular docking studies. The

recent emergence of pharmaceutical cocrystals,³ which exploit noncovalent interactions (i.e., hydrogen bonding) for the supramolecular synthesis of multiple component crystalline materials suitable for therapeutic use, may also be regarded as *supramolecular medicinal chemistry*; however, thus far, it has only managed to gain industrial recognition during formulation studies.

In the context of supramolecular synthesis there exist two primary design elements: noncovalent hydrogen bonds and coordinative covalent bonds. It should, therefore, be unsurprising that the exploitation of coordinative covalent bonding to generate multiple component crystalline materials suitable for therapeutic use has also been explored.⁴ Particularly, we have recently reported that the supramolecular synthesis of mixed-ligand metal complexes that possess active pharma-

* To whom correspondence should be addressed. Mailing address: Department of Chemistry, Brown University, 324 Brook St., Providence, RI 02912. Phone: 401-863-3775. Fax: 401-863-9046. E-mail: brian_moulton@brown.edu.

- (1) Lehn, J. M. Supramolecular Chemistry—Scope and perspectives molecules, supermolecules, and molecular devices. *Angew. Chem., Int. Ed. Engl.* **1988**, 27, 89–112. Moulton, B.; Zaworotko, M. J. From molecules to crystal engineering. Supramolecular isomerism and polymorphism in network solids. *Chem. Rev.* **2001**, 101, 1629–1658. Aakeroy, C. B.; Desper, J.; Smith, M.; Urbina, J. F. [(Benzimidazol-1-yl)methyl]benzamides as bifunctional reagents for reliable inorganic-organic supramolecular synthesis. *Dalton Trans.* **2005**, 2462–2470.
- (2) Smith, D. K. A Supramolecular Approach to Medicinal Chemistry: Medicine Beyond the Molecule. *J. Chem. Educ.* **2005**, 82, 393–400.

- (3) Vishweshwar, P.; McMahon, J. A.; Bis, J. A.; Zaworotko, M. J. Pharmaceutical co-crystals. *J. Pharm. Sci.* **2006**, 95, 499–516. Trask, A. V.; Samuel Mother Well, W. D.; Jones, W. Pharmaceutical Cocrystallization: Engineering a Remedy for Caffeine Hydration. *Cryst. Growth Des.* **2005**, 5, 1013–1021. Reddy, L. S.; Babu, N. J.; Nangia, A. Carboxamide-pyridine N-oxide heterosynthon for crystal engineering and pharmaceutical cocrystals. *Chem. Commun.* **2006**, 1369–1371. Almarsson, O.; Zaworotko, M. J. Crystal engineering of the composition of pharmaceutical phases. Do pharmaceutical co-crystals represent a new path to improved medicines? *Chem. Commun.* **2004**, 1889–1896.

ceutical ingredients (APIs)⁵ as ligands offers a complementary approach to the synthesis of pharmaceutical cocrystals for affecting key therapeutic parameters such as solubility and lipophilicity.

Although uses of metals for medicinal purposes have been known for centuries, recent developments of metals in medicine have focused primarily on metal-based drugs and metal-based diagnostic agents such as magnetic resonance imaging (MRI) contrast agents and radiopharmaceuticals.⁶ Many metal complexes with good therapeutic effect have been reported.⁷ For instance, numerous Cu(II) complexes of nonsteroidal anti-inflammatory drugs (NSAIDs) exhibit enhanced anti-inflammatory activity and reduced gastrointestinal toxicity compared with their parent NSAIDs.⁸

In the context of transition metal complexes, there are two classifications of ligands: neutral and charge-compensating (i.e., anionic). There are, therefore, three primary classes of mixed-ligand pharmaceutical coordination species: anionic API with neutral ancillary ligand, anionic ancillary ligand with neutral API, and species with both anionic API and ancillary ligand (the latter may, or may not, have additional neutral ancillary ligands, such as solvent molecules). Herein we describe the synthesis and characterization of examples of all three classes of complexes and report their bulk solubility in water and octanol, solubility ratio, and partition coefficient.

Experimental Section

Materials. 1-Octanol (ACS reagent, ≥99%) was ordered from Aldrich Chemical Co. Deionized water with resistivity up to 18.3 MΩ/cm was prepared by a NANOpure Ultrapure Water System. All other materials were obtained from Aldrich Chemical Co. or VWR International Inc. and used as received.

Methods. Single-crystal X-ray diffraction data were collected on a BRUKER SMART-APEX CCD diffractometer using Mo Kα radiation ($\lambda = 0.71073$ Å). Thermogravimetric analysis was performed under nitrogen on TA instruments

TGA Q500 Hi-Res. XRPD data were collected on a Bruker D8 diffractometer at 40 kV, 40 mA for Cu Kα ($\lambda = 1.5418$ Å), with a step size 0.01° in 2θ at room temperature. UV–vis spectra were recorded on a HP 8452A diode array UV–vis spectrometer. ESI (electrospray ionization)–MS spectra were recorded on an Applied Biosystem QSTAR instrument. IR spectra were recorded on an ATI Mattson Infinity series FTIR instrument. NMR spectra were obtained on a Bruker Avance 400 spectrometer.

NMR tubes with a 5 mm internal diameter were used. The diffusion NMR experiment was performed at 298 K with a stimulated echo sequence (STE) using bipolar gradient pulse pair. Diffusion coefficients were measured by incrementing the amplitude of the field gradient pulse over 32 steps (0.5–30 G/cm). The bipolar gradient duration and the diffusion time were optimized to 2.4 and 14.9 ms, respectively. The intensities were fitted to an exponential decay using the *SimFit* program within the Topspin software to provide estimates of the diffusion constant.

Measurement of P . Partition coefficients of complexes were determined in a 1-octanol/water system. 1-Octanol and water were mutually saturated before use. The octanol-saturated water (ow) layer was used to prepare the stock solution, generally 25 mL of which was stirred vigorously, in triplicate, with 50 mL of water-saturated octanol (wo) at 25 °C overnight. The organic layer was collected, and centrifuged at 7000 rpm for 20 min to get rid of a trace amount of water. The organic layer was analyzed by UV. The partition coefficient was determined from eq 1,

$$P = \frac{C_{wo}}{(m - C_{wo}V_{wo})/V_{ow}} \quad (1)$$

where m represents the total mass of the sample; C_{wo} represents equilibrium solute concentrations of the octanol phase; V_{ow} and V_{wo} represent the volume of aqueous and octanol phases, respectively.

The only exception is the measurement of P of copper acetate monohydrate ($\text{Cu}_2(\text{CH}_3\text{COO})_4(\text{H}_2\text{O})_2$). The octanol-saturated layer was collected. Then an extra amount of $\text{NH}_4\text{-OH}$ solution was added and mixed well. The mixture was analyzed by UV–vis at 615 nm. The partition coefficient was determined from eq 2.

$$P = \frac{(m - C_{ow}V_{ow})/V_{wo}}{C_{ow}} \quad (2)$$

Measurement of Solubility. Solubilities were determined at 25 °C in water (S_w), octanol-saturated water (S_{ow}), and water-saturated octanol (S_{wo}). An excess of the sample was added to 15 mL of each solvent and stirred vigorously at 25 °C for 8 h. This was then ported immediately into centrifuge tubes and centrifuged at 7000 rpm for 20 min. The supernatant was collected. The supernatant samples after appropriate dilutions with respective solvent were analyzed by UV spectrometry using a standard plot of solute in the same medium. The solubility of copper acetate in water-saturated octanol was determined by extracting 200 mL of

- (4) Farrel, N. *Transition Metal Complexes as Drugs and Chemotherapeutic Agents*; Kluwer: Dordrecht, The Netherlands, 1989.
- (5) Sorenson, J. R. J. Copper complexes—a unique class of anti-arthritis drugs. *Prog. Med. Chem.* **1978**, *15*, 211–260.
- (6) Ma, Z.; Moulton, B. Mixed-ligand coordination species: a promising approach for “second-generation” drug development. *Cryst. Growth Des.* **2007**, *7*, 196–198.
- (7) Guo, Z.; Sadler, P. J. Metals in Medicine. *Angew. Chem., Int. Ed.* **1999**, *38*, 1512–1531.
- (8) Lippert, B. *Cisplatin—Chemistry and Biochemistry of a Leading Anticancer Drug*; Wiley-VCH: Weinheim, 1999.
- (9) Schmidbaur, H. *Gold—Progress in Chemistry, Biochemistry and Technology*; Wiley: New York, 1999.
- (10) Milanino, R.; Rainsford, K. D.; Velo, G. P. *Copper and Zinc in Inflammation*; Kluwer: Dordrecht, 1989.
- (11) Weder, J. E.; Dillon, C. T.; Hambley, T. W.; Kennedy, B. J.; Lay, P. A.; Biffin, J. R.; Regtop, H. L.; Davies, N. M. Copper complexes of non-steroidal anti-inflammatory drugs: an opportunity yet to be realized. *Coord. Chem. Rev.* **2002**, *232*, 95–126.

saturated wo solution into 20 mL of ow solution. Then the aqueous (ow) layer was analyzed by UV–vis at 615 nm after addition of the proper amount of NH_4OH solution.

Synthesis and Characterization of Mixed-Ligand Cu(II) Complexes. The structures of the 28 mixed-ligand Cu(II) complexes are listed in Figure 1.

Complexes ASP-(1–9). We have previously synthesized and characterized complexes ASP-(1–9).⁵

Complexes SAS-(1–9). CCDC 639399–639406 (SAS-(2–9)) contain the supplementary crystallographic data for this paper. These data can be obtained free of charge from the Cambridge Crystallographic Data Center via www.ccdc.cam.ac.uk/data_request/cif. Powder XRD patterns of complexes SAS-(1–9) are listed in Figure 2.

Complex SAS-1. Experimental procedures to prepare polycrystalline $\text{Cu}_2(\text{SAS})_4(\text{water})_2$ have been previously detailed.²⁸ Hi-Res TGA: peak 120.06 °C, weight loss 5.759%; peak 213.38 °C, 282.78 °C, 374.54 °C, weight loss 75.73%.

Complex SAS-2. $\text{Cu}_2(\text{SAS})_4(\text{caffeine})_2$ was prepared by adding 0.5 g of $\text{Cu}_2(\text{SAS})_4(\text{water})_2$ and 0.163 g of caffeine into 10 mL of AcCN in a 4 dram glass vial. The mixture was placed in a water bath at 60 °C for 1 h and then set aside. After 1 day, a green crystal was formed. Hi-Res TGA: peak 214.27 °C, weight loss 48.53%; peak 269.77 °C, weight loss 38.69%. Crystal data: $\text{C}_{72}\text{H}_{56}\text{Cu}_2\text{N}_8\text{O}_{24}$, $M = 1544.33$, monoclinic, $P2_1/n$, $a = 12.904(2)$ Å, $b = 17.095(3)$ Å, $c = 15.923(3)$ Å, $\beta = 109.361(4)^\circ$, $V = 3313.9(11)$ Å³, $Z = 2$, $\mu(\text{Mo K}\alpha) = 0.734$ mm^{−1}, $T = 90(2)$ K, $R1 = 0.0662$, $wR2 = 0.1370$.

Complex SAS-3. $\text{Cu}_2(\text{SAS})_4(3\text{-Cl-Py})_2$ was prepared by adding 3-Cl-Py to 0.5 g of $\text{Cu}_2(\text{SAS})_4(\text{water})_2$ until the solid was merged by 3-Cl-Py in a 4 dram glass vial. The mixture was placed in a water bath at 60 °C for 1 h and then set aside. After 1 day, a green crystal was formed. Hi-Res TGA: peak 172.29 °C, 199.14 °C, 279.59 °C, weight loss 81.86%. Crystal data: $\text{C}_{66}\text{H}_{44}\text{Cl}_2\text{Cu}_2\text{N}_2\text{O}_{20}$, $M = 1383.01$, triclinic, $P\bar{1}$, $a = 10.423(18)$ Å, $b = 11.032(18)$ Å, $c = 14.32(2)$ Å, $\alpha = 104.03(3)^\circ$, $\beta = 94.41(3)^\circ$, $\gamma = 108.91(4)^\circ$, $V = 1490(4)$ Å³, $Z = 1$, $\mu(\text{Mo K}\alpha) = 0.886$ mm^{−1}, $T = 90(2)$ K, $R1 = 0.1151$, $wR2 = 0.2621$. The crystal of complex SAS-3 is tiny and the diffraction was weak, which resulted in a relatively high R value.

Complex SAS-4. $\text{Cu}_2(\text{SAS})_4(4\text{-Bz-Py})_2$ was prepared by adding 5 drops of 4-benzylpyridine and 0.2 g of $\text{Cu}_2(\text{SAS})_4(\text{water})_2$ into 5 mL of THF in a 4 dram glass vial. The mixture was placed in a water bath at 60 °C for 1 h and then set aside. After 1 day, a green crystal was formed. Hi-Res TGA: peak 186.25 °C, 215.66 °C, 265.90 °C, weight loss 85.37%. Crystal data: $\text{C}_{80}\text{H}_{58}\text{Cu}_2\text{N}_2\text{O}_{20}$, $M = 1494.36$, triclinic, $P\bar{1}$, $a = 10.209(3)$ Å, $b = 11.122(3)$ Å, $c = 14.977(4)$ Å, $\alpha = 98.475(6)^\circ$, $\beta = 99.077(5)^\circ$, $\gamma = 94.780(6)^\circ$, $V = 1494.36$ Å³, $Z = 1$, $\mu(\text{Mo K}\alpha) = 0.727$ mm^{−1}, $T = 90(2)$ K, $R1 = 0.0697$, $wR2 = 0.1899$.

Complex SAS-5. $\text{Cu}_2(\text{SAS})_4(4\text{-Ph-Py})_2(\text{THF})_2$ was prepared by adding 0.05 g of 4-phenylpyridine and 0.2 g of $\text{Cu}_2(\text{SAS})_4(\text{water})_2$ into 5 mL of THF in a 4 dram glass vial.

The mixture was placed in a water bath at 60 °C for 1 h and then set aside. After 1 day, a green crystal was formed. Hi-Res TGA: peak 126.08 °C, weight loss 10.02%; peak 209.15 °C, 299.94 °C, weight loss 76.94%. Crystal data: $\text{C}_{78}\text{H}_{54}\text{Cu}_2\text{N}_2\text{O}_{20}(\text{C}_4\text{H}_8\text{O})_2$, $M = 1610.52$, monoclinic, $C2/c$, $a = 28.910(10)$, $b = 12.621(4)$, $c = 41.649(15)$ Å, $\beta = 92.434(8)^\circ$, $V = 15182(9)$ Å³, $Z = 8$, $\mu(\text{Mo K}\alpha) = 0.640$ mm^{−1}, $T = 90(2)$ K, $R1 = 0.0819$, $wR2 = 0.1915$.

Complex SAS-6. $\text{Cu}(\text{SAS})_2(\text{Py})_3$ was prepared by adding pyridine to 0.5 g of $\text{Cu}_2(\text{SAS})_4(\text{water})_2$ until the solid was merged by pyridine in a 4 dram glass vial. The mixture was placed in a water bath at 60 °C for 1 h and then set aside. After 1 day, a blue crystal was formed. Hi-Res TGA: peak 98.73 °C, 202.39 °C, 306.63 °C, weight loss 85.35%. Crystal data: $\text{C}_{43}\text{H}_{33}\text{CuN}_3\text{O}_{10}$, $M = 815.26$, monoclinic, $C2/c$, $a = 23.694(3)$ Å, $b = 9.3561(12)$ Å, $c = 16.664(2)$ Å, $\beta = 97.587(3)^\circ$, $V = 3661.8(8)$ Å³, $Z = 4$, $\mu(\text{Mo K}\alpha) = 0.664$ mm^{−1}, $T = 90(2)$ K, $R1 = 0.0518$, $wR2 = 0.0942$.

Complex SAS-7. $\text{Cu}_2(\text{SAS})_4(\text{water})_2$ (0.4 g) was stirred vigorously and suspended in 10 mL of THF. The suspension was then transferred to an 8 dram glass vial. An AcCN solution of isonicotinamide (20 mL, 0.1 mol/L) was carefully added into the vial. Purple crystals $\text{Cu}(\text{SAS})_2(\text{isonicotinamide})_2(\text{AcCN})_{2/3}$ formed within a week under ambient conditions. Hi-Res TGA: peak 149.72 °C, 185.00 °C, weight loss 84.32%. Crystal data: $(\text{C}_{40}\text{H}_{30}\text{CuN}_4\text{O}_{12})_3(\text{C}_2\text{H}_3\text{N})_2$, $M = 2548.77$, triclinic, $P\bar{1}$, $a = 12.415(3)$ Å, $b = 12.601(3)$ Å, $c = 20.925(4)$ Å, $\alpha = 90.47(3)^\circ$, $\beta = 97.14(3)^\circ$, $\gamma = 118.31(3)^\circ$, $V = 2850.9(10)$ Å³, $Z = 1$, $\mu(\text{Mo K}\alpha) = 0.648$ mm^{−1}, $T = 90(2)$ K, $R1 = 0.0605$, $wR2 = 0.1652$.

Complex SAS-8. $\text{Cu}(\text{SAS})_2(4\text{-Me-Py})_2$ was prepared by adding 4-methylpyridine to 0.5 g of $\text{Cu}_2(\text{SAS})_4(\text{water})_2$ until the solid was merged by 4-methylpyridine in a 4 dram glass vial. The mixture was placed in a water bath at 60 °C for 1 h and then set aside. After 1 day, the purple crystal was formed. Hi-Res TGA: peak 142.34 °C, 206.39 °C, 283.10 °C, weight loss 85.12%. Crystal data: $\text{C}_{40}\text{H}_{32}\text{CuN}_2\text{O}_{10}$, $M = 764.22$, monoclinic, $P2_1/n$, $a = 7.8154(16)$, $b = 15.567(3)$, $c = 14.920(3)$ Å, $\beta = 104.52(3)^\circ$, $V = 1757.2(6)$ Å³, $Z = 2$, $\mu(\text{Mo K}\alpha) = 0.686$ mm^{−1}, $T = 90(2)$ K, $R1 = 0.0505$, $wR2 = 0.0904$.

Complex SAS-9. $\text{Cu}(\text{SAS})_2(4\text{-Et-Py})_2$ was prepared by adding 4-ethylpyridine to 0.5 g of $\text{Cu}_2(\text{SAS})_4(\text{water})_2$ until the solid was merged by 4-ethylpyridine in a 4 dram glass vial. The mixture was placed in a water bath at 60 °C for 1 h and then set aside. After 1 day, the purple crystal was formed. Hi-Res TGA: 148.55 °C, 203.68 °C, 266.73 °C, weight loss 88.23%. Crystal data: $\text{C}_{42}\text{H}_{36}\text{CuN}_2\text{O}_{10}$, $M = 792.27$, monoclinic, $P2_1/n$, $a = 7.822(3)$, $b = 15.493(6)$, $c = 15.188(5)$ Å, $\beta = 102.096(8)^\circ$, $V = 1799.7(11)$ Å³, $Z = 2$, $\mu(\text{Mo K}\alpha) = 0.672$ mm^{−1}, $T = 90(2)$ K, $R1 = 0.0610$, $wR2 = 0.1200$.

Complexes MC-(2–5). Experimental procedures to prepare MC-(2–5) have been previously detailed. Powder XRD patterns of complexes MC-(2–5) are listed in Figure 3.

Complex MC-2. Hi-Res TGA: peak 166.26 °C, 233.89 °C, weight loss 76.82%.

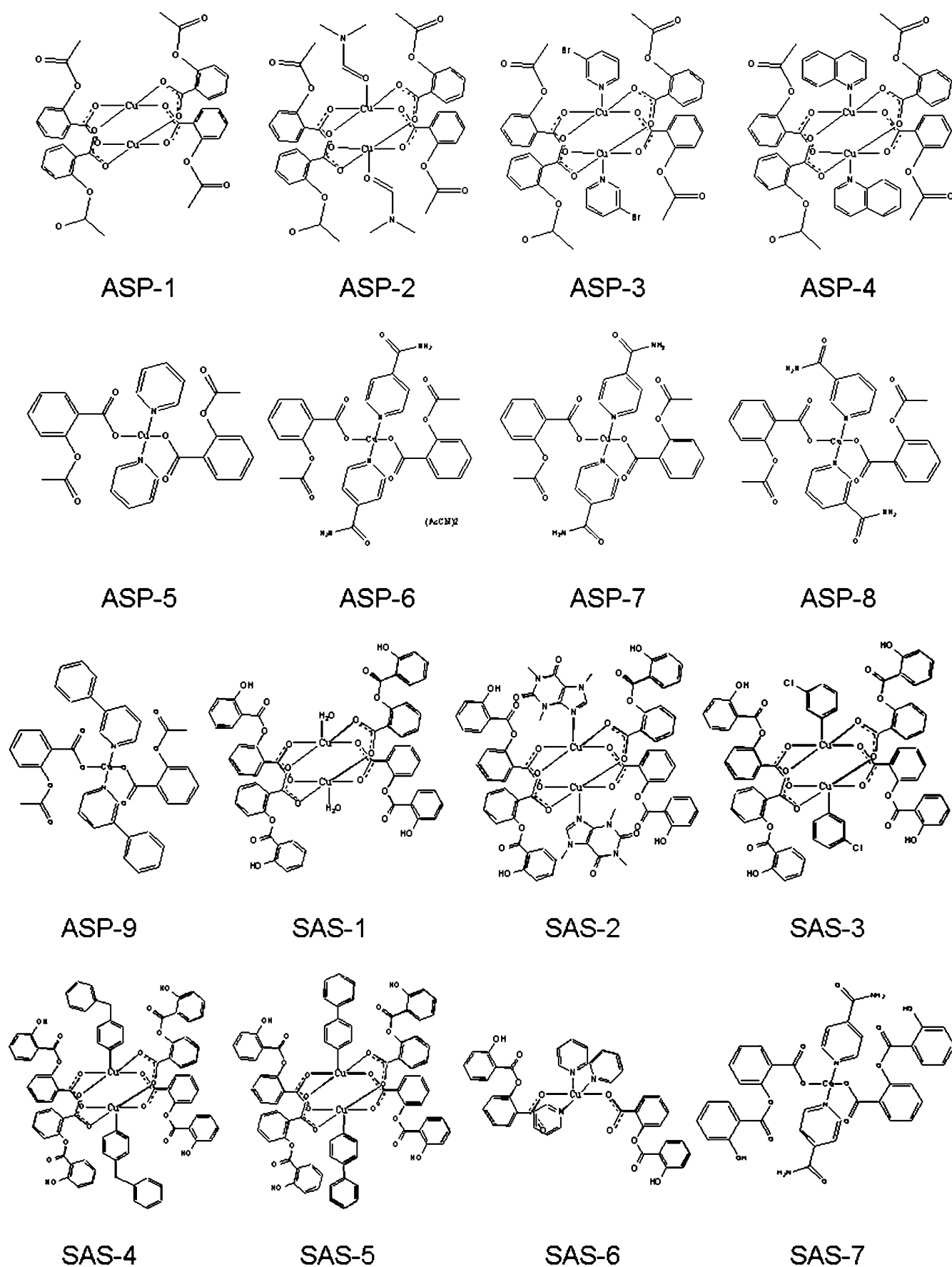


Figure 1 (Continued)

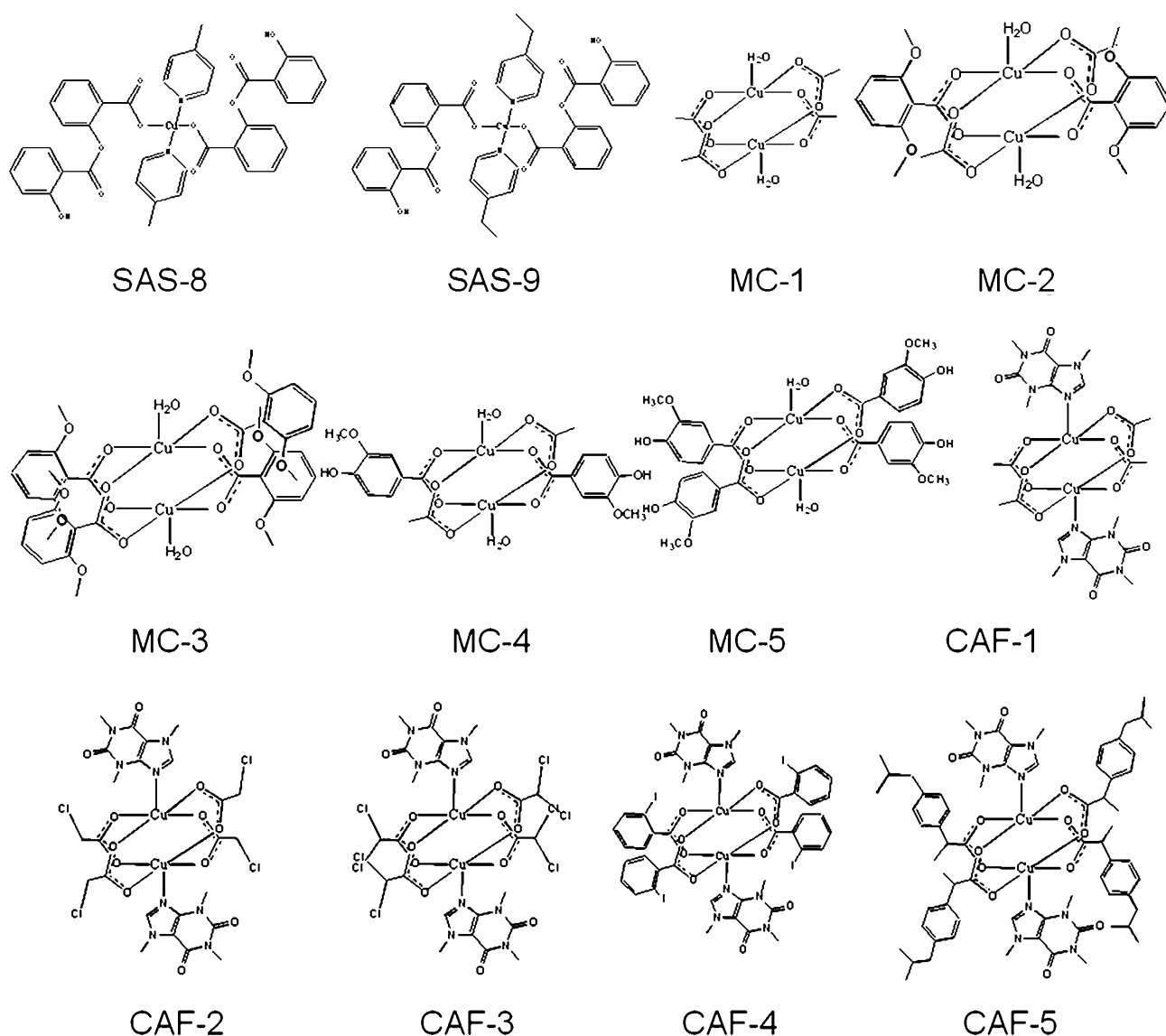


Figure 1. Structures of the 28 mixed-ligand copper(II) coordination complexes (abbreviations: **ASP**, aspirin and copper(II)–aspirinate complexes; **SAS**, salicylate and copper(II)–salicylate complexes; **MC**, mixed carboxylate copper(II) complexes; **CAF**, caffeine and copper(II) carboxylate–caffeine complexes).

Complex MC-3. Hi-Res TGA: peak 132.21 °C, 200.87 °C, weight loss 74.65%.

Complex MC-4. Hi-Res TGA: peak 51.72 °C, 152.12 °C, 217.27 °C, 230.57 °C, 258.49 °C, 325.52 °C, weight loss 64.95%.

Complex MC-5. Hi-Res TGA: peak 189.64 °C, weight loss 38.92%; peak 294.52 °C, weight loss 40.19%.

Complexes CAF-(1–5). Experimental procedures to prepare **CAF-(1–5)** have been previously detailed.^{29–31} Powder XRD patterns of complexes **CAF-(1–5)** are listed in Figure 4.

Complex CAF-1. Hi-Res TGA: peak 206.58 °C, 246.76 °C, 358.51 °C, weight loss 78.76%. IR (KBr): 1624 cm^{-1} s (ν_{COO^-} (asym)); 1422 cm^{-1} m (ν_{COO^-} (sym)).

Complex CAF-2. Hi-Res TGA: peak 193.03 °C, weight loss 71.15%. IR (KBr): 1650 cm^{-1} s (ν_{COO^-} (asym)); 1413 cm^{-1} m (ν_{COO^-} (sym)).

Complex CAF-3. Hi-Res TGA: peak 184.98 °C, 199.66 °C, 221.81 °C, weight loss 78.71%. IR (KBr): 1650 cm^{-1} s (ν_{COO^-} (asym)); 1401 cm^{-1} m (ν_{COO^-} (sym)).

Complex CAF-4. Hi-Res TGA: peak 233.08 °C, 305.58 °C, weight loss 57.07%. IR (KBr): 1628 cm^{-1} s (ν_{COO^-} (asym)); 1405 cm^{-1} s (ν_{COO^-} (sym)).

Complex CAF-5. Hi-Res TGA: peak 201.92 °C, 236.21 °C, 363.84 °C, weight loss 88.92%. IR (KBr): 1662 cm^{-1} s (ν_{COO^-} (asym)); 1405 cm^{-1} m (ν_{COO^-} (sym)).

Results

Recently, we introduced the concept that the lipophilicity and solubility of Cu(II)–aspirin complexes can be tuned by varying the nature of a neutral ancillary ligand.⁵ In this work, comprehensive studies have been done: four series of complexes were prepared and summarized (including the Cu–aspirin species) in Table 1. The coordination chro-

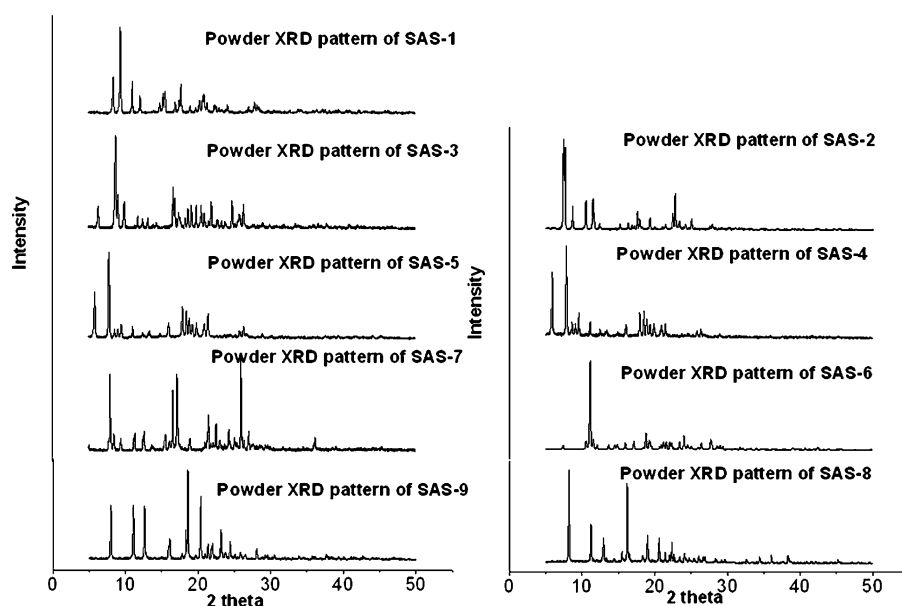


Figure 2. Powder XRD pattern of complexes **SAS-(1–9)**.

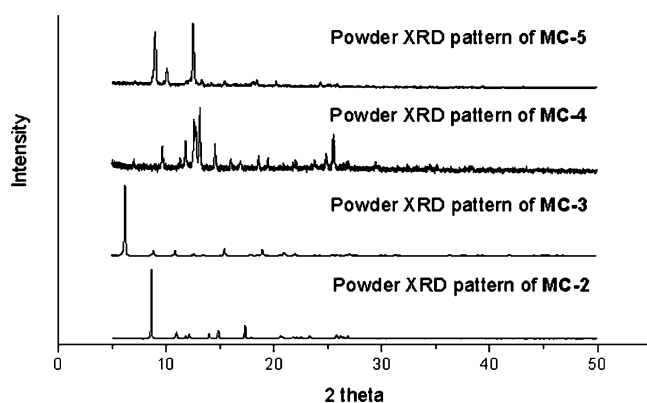


Figure 3. Powder XRD patterns of complexes **MC-(2–5)**.

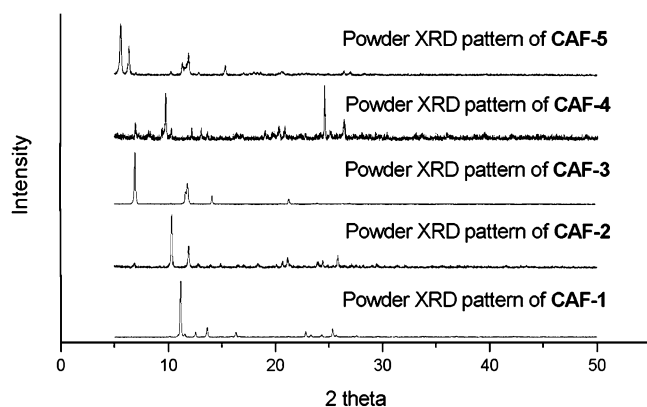


Figure 4. Powder XRD patterns of complexes **CAF-(1–5)**.

mophore of these complexes is illustrated in Figure 5. Tables 2–5 list their respective solubilities in water (S_w), octanol-saturated water (S_{ow}), and water-saturated octanol (S_{wo}) at 25 °C. The partition coefficient ($\log P$) and solubility ratio $\log SR$ ($\log (S_{wo}/S_{ow})$) for each compound have also been listed in Tables 2–5. $\log P$ and $\log SR$ are commonly used

as a suitable estimate of lipophilicity.⁹ The additive–constitutive character of partition coefficients within a congeneric series of compounds prepared from a parent organic drug is well established.¹⁰ More specifically, inductive effect, resonance effect, and hydrogen bond are important factors that affect lipophilicity.¹¹ Herein, we undertook a systematic effort toward understanding *in vitro* quantitative structure–activity relationships (QSAR) for metal–drug complexes.

As mentioned in the Introduction, the 28 Cu(II) complexes can be classified into 3 categories: (1) (anionic active pharmaceutical ingredient)–Cu(II)–(neutral ancillary ligand), specifically, Cu(II)–(aspirin)–(AL) and Cu(II)–(salsalate)–(AL) were studied as model species; (2) (anionic active pharmaceutical ingredient)–Cu(II)–(anionic ancillary ligand), specifically, mixed carboxylate Cu(II) species were chosen for study; (3) (neutral active pharmaceutical ingredient)–Cu(II)–(anionic ancillary ligand), specifically, carboxylate–Cu(II)–caffeine species were studied as model species. Detailed experimental data have been described herein.

- (9) Yalkowsky, S. H.; Valvani, S. C.; Roseman, T. J. Solubility and partitioning VI: octanol solubility and octanol–water partition coefficients. *J. Pharm. Sci.* **1983**, *72*, 866–870. Pinsuwan, S.; Li, A.; Yalkowsky, S. H. Correlation of Octanol/Water Solubility Ratios and Partition Coefficients. *J. Chem. Eng. Data* **1995**, *40*, 623–626. Jozan, M.; Takacs-Novak, K. Determination of solubilities in water and 1-octanol of nitrogen-bridgehead heterocyclic compounds. *Int. J. Pharm.* **1997**, *159*, 233–242.
- (10) Fujita, T.; Iwasa, J.; Hansch, C. A New Substituent Constant, π , Derived from Partition Coefficients. *J. Am. Chem. Soc.* **1964**, *86*, 5175–5180.
- (11) Leo, A.; Hansch, C.; Elkins, D. Partition coefficients and their uses. *Chem. Rev.* **1971**, *71*, 525–616.
- (12) Koch, P. A.; Schultz, C. A.; Wills, R. J.; Hallquist, S. L.; Welling, P. G. Influence of food and fluid ingestion on aspirin bioavailability. *J. Pharm. Sci.* **1978**, *67*, 1533–1535.

Table 1. Formulas and Coordination Chromophores of the 28 Cu(II) Complexes in the Current Work

complex no.	complex formula	coordination chromophore
ASP-1	Cu ₂ (ASP) ₄	4-coordinate paddle wheel
ASP-2	Cu ₂ (ASP) ₄ (DMF) ₂	5-coordinate paddle wheel
ASP-3	Cu ₂ (ASP) ₄ (3-Br-Py) ₂	5-coordinate paddle wheel
ASP-4	Cu ₂ (ASP) ₄ (quinoline) ₂	5-coordinate paddle wheel
ASP-5	Cu(ASP) ₂ (pyridine) ₂	4-coordinate square planar
ASP-6	Cu(ASP) ₂ (isonicotinamide) ₂ (AcCN) ₂	4-coordinate square planar
ASP-7	Cu(ASP) ₂ (isonicotinamide) ₂	4-coordinate square planar
ASP-8	Cu(ASP) ₂ (nicotinamide) ₂	4-coordinate square planar
ASP-9	Cu(ASP) ₂ (3-phenylpyridine) ₂	4-coordinate square planar
SAS-1	Cu ₂ (SAS) ₄ (H ₂ O) ₂	5-coordinate paddle wheel
SAS-2	Cu ₂ (SAS) ₄ (caffeine) ₂	5-coordinate paddle wheel
SAS-3	Cu ₂ (SAS) ₄ (3-chloropyridine) ₂	5-coordinate paddle wheel
SAS-4	Cu ₂ (SAS) ₄ (4-benzylpyridine) ₂	5-coordinate paddle wheel
SAS-5	Cu ₂ (SAS) ₄ (4-phenylpyridine) ₂ (THF) ₂	5-coordinate paddle wheel
SAS-6	Cu(SAS) ₂ (pyridine) ₃	5-coordinate square pyramidal
SAS-7	Cu(SAS) ₂ (isonicotinamide) ₂ (AcCN) _{2/3}	4-coordinate square planar
SAS-8	Cu(SAS) ₂ (4-methylpyridine) ₂	4-coordinate square planar
SAS-9	Cu(SAS) ₂ (4-ethylpyridine) ₂	4-coordinate square planar
MC-1	Cu ₂ (CH ₃ COO) ₄ (H ₂ O) ₂	5-coordinate paddle wheel
MC-2	Cu ₂ (CH ₃ COO) ₂ (DMB) ₂ (H ₂ O) ₂	5-coordinate paddle wheel
MC-3	Cu ₂ (DMB) ₄ (H ₂ O) ₂	5-coordinate paddle wheel
MC-4	Cu ₂ (CH ₃ COO) ₂ (VA) ₂ (H ₂ O) ₂	5-coordinate paddle wheel
MC-5	Cu ₂ (VA) ₄ (H ₂ O) ₂	5-coordinate paddle wheel
CAF-1	Cu ₂ (CH ₃ COO) ₄ (caffeine) ₂	5-coordinate paddle wheel
CAF-2	Cu ₂ (ClCH ₂ COO) ₄ (caffeine) ₂	5-coordinate paddle wheel
CAF-3	Cu ₂ (Cl ₂ CHCOO) ₄ (caffeine) ₂	5-coordinate paddle wheel
CAF-4	Cu ₂ (2-iodobenzoato) ₄ (caffeine) ₂	5-coordinate paddle wheel
CAF-5	Cu ₂ (ibuprofen) ₄ (caffeine) ₂	5-coordinate paddle wheel

Anionic API with Neutral AL. Compounds containing nonsteroidal anti-inflammatory drugs (NSAIDs) as ligands in copper(II) complexes are known; indeed, they have been shown to exhibit both enhanced efficacy and reduced side effects.⁸ Aspirin (ASP)/salsalate (SAS) and a representative group of ancillary ligands were selected to form mixed-ligand copper(II) coordination species, respectively.

The partition coefficient (log *P*) and solubility ratio (log SR) for each compound for these two series have been shown graphically in Figures 6 and 7, respectively. For the binuclear Cu(II)–aspirinate species, log *P* and log SR values were significantly increased via the introduction of both 3-bromopyridine and quinoline. The order of log *P*/log SR values for the dicopper complexes, Cu₂(ASP)₄(AL)₂, reflects the

order of log *P* values calculated for the ancillary ligands (Figure 6), which is consistent with the additive–constitutive character observed for organic congeners. For the mononuclear Cu(II)–aspirinate species, a similar general tendency is observed, the exception being that, although the log *P* values of isonicotinamide and nicotinamide are smaller than that of pyridine, the SR values for complexes ASP-(6–8) are close to the SR value for ASP-5; moreover, the log *P* values are greater. This indicates that the lipophilicity of complexes ASP-(6–8) is greater than expected based on the log *P* value of the ancillary ligand. This is attributed to hydrogen bonding, which is consistent with the additive–constitutive character of hydrogen-bonding functionalities in metal-free solid forms where it has been suggested that hydrogen bonding reduces the affinity for the aqueous phase and thus increases the relative lipophilicity.¹³ In comparing the binuclear and mononuclear Cu(II)–aspirinate species, the complexes that possess the dicopper chromophore are more lipophilic than the mononuclear complexes. ESI-MS of complexes ASP-(5,6,8) suggest that the

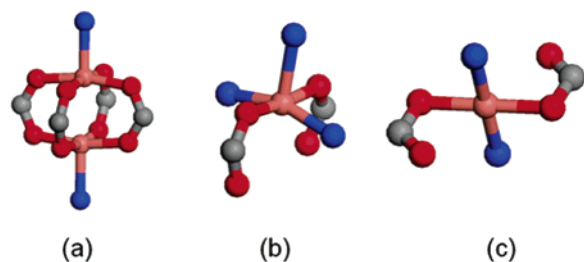


Figure 5. Schematic illustration of coordination chromophore of Cu(II) complexes. (a): 5-coordinate paddle wheel; (b) 5-coordinate square pyramidal; (c) 4-coordinate square planar.

- (13) Silverman, R. B. *The Organic Chemistry of Drug Design and Drug Action.*; Academic Press: Longdon, 1992; pp 30–31. Charton, M.; Charton, B. I. Hydrogen bonding contribution to lipophilicity parameters. Hydrogen acceptor and hydrogen donor parameters. *Collect. Czech. Chem. Commun.* **2004**, 69, 2147–2173.

Table 2. Solubilities, Solubility Ratios, and Partition Coefficients of Aspirin and Complexes **ASP-(1–9)** at 25 °C

	log <i>P</i> of AL ^a	<i>S_w</i> (mg/mL)	<i>S_{ow}</i> (mg/mL)	<i>S_{wo}</i> (mg/mL)	log SR (<i>S_{wo}</i> / <i>S_{ow}</i>)	log <i>P</i> of complex
aspirin (ASP)		4.600 ^b	4.295(10)	54.16(94)	1.101	1.321(25)
ASP-1		3.414(25)	2.981(3)	0.9767(36)	−0.4847	−0.2371(267)
ASP-2	−1.010(277)	3.092(33)	4.493(4)	1.463(26)	−0.4873	−0.3484(166)
ASP-3	1.751(286)	1.564(3)	1.566(5)	1.256(15)	−0.09583	0.1066(58)
ASP-4	2.084(195)	2.729(1)	3.342(3)	5.460(23)	0.2133	0.4772(140)
ASP-5	0.726(178)	3.425(21)	3.629(24)	1.210(47)	−0.4770	−0.7001(111)
ASP-6	−0.282(289)	9.315(10)	5.767(7)	1.832(17)	−0.4980	−0.4647(274)
ASP-7	−0.282(289)	9.259(5)	5.654(20)	1.673(9)	−0.5333	−0.4723(272)
ASP-8	−0.110(237)	4.417(50)	3.361(29)	0.7541(97)	−0.6490	−0.5257(136)
ASP-9	2.600(244)	0.5415(7)	0.4085(17)	1.150(20)	0.4495	0.9106(312)

^a log *P* values of ancillary ligands were calculated using Advanced Chemistry Development (ACD/Labs) Software V8.14 for Solaris. ^b From ref 12.

Table 3. Solubilities, Solubility Ratios, and Partition Coefficients of Salsalate and Complexes **SAS-(1–9)** at 25 °C

	log <i>P</i> of AL ^a	<i>S_w</i> (mg/mL)	<i>S_{ow}</i> (mg/mL)	<i>S_{wo}</i> (mg/mL)	log SR (<i>S_{wo}</i> / <i>S_{ow}</i>)	log <i>P</i> of complex
salsalate (SAS)		0.59 ^a	0.59 ^b	87.83(38)	2.176	3.045(353) ^a
SAS-1		0.2791(6)	0.2962(10)	3.200(5)	1.033	0.06927(1394)
SAS-2	−0.131(371)	0.3405(20)	0.3227(6)	0.6516(100)	0.3051	0.05420(695)
SAS-3	1.569(214)	0.1239(1)	0.1259(4)	0.7034(61)	0.7472	0.06467(1468)
SAS-4	2.715(199)	0.0134(3)	0.0153(3)	0.3314(22)	1.336	0.7481(870)
SAS-5	2.590(242)	0.0303(3)	0.0315(2)	1.236(18)	1.593	1.231(53)
SAS-6	0.726(178)	0.4065(8)	0.3291(8)	1.918(5)	0.7655	0.03218(199)
SAS-7	−0.282(289)	0.3143(9)	0.2890(10)	0.8344(165)	0.4241	0.03802(967)
SAS-8	1.186(185)	0.2301(18)	0.2174(10)	1.932(23)	0.9488	0.01407(1658)
SAS-9	1.718(185)	0.1143(2)	0.1104(8)	1.438(9)	1.115	0.02089(576)

^a log *P* of ancillary ligands/salsalate and water solubility of salsalate were calculated using Advanced Chemistry Development (ACD/Labs) Software V8.14 for Solaris. ^b *S_{ow}* and *S_w* of salsalate were supposed to be equal.

Table 4. Solubilities, Solubility Ratios and Partition Coefficients of Complexes **MC-(1–5)** at 25 °C

	<i>S_w</i> (mg/mL)	<i>S_{ow}</i> (mg/mL)	<i>S_{wo}</i> (mg/mL)	log SR (<i>S_{wo}</i> / <i>S_{ow}</i>)	log <i>P</i> of complex
MC-1	72 ^a	74.47(136)	0.1161(438)	−2.807	−2.222(553)
MC-2	15.82(11)	15.64(14)	0.5841(103)	−1.428	−1.496(15)
MC-3	33.61(21)	31.97(19)	3.872(125)	−0.9168	−1.442(27)
MC-4	0.1257(12)	0.1257(12)	0.1257(12)	0.6573	−0.6626(353)
MC-5	0.1257(12)	0.1257(12)	0.1257(12)	−1.081	0.0928(3389)

^a *S_w* of Cu₂(Ac)₄(H₂O)₂ is from MSDS.

Table 5. Solubilities, Solubility Ratios, and Partition Coefficients of Caffeine and Complexes **CAF-(1–5)** at 25 °C

	log <i>P</i> of H(AL) ^a	<i>S_w</i> (mg/mL)	<i>S_{ow}</i> (mg/mL)	<i>S_{wo}</i> (mg/mL)	log SR (<i>S_{wo}</i> / <i>S_{ow}</i>)	log <i>P</i> of complex
caffeine(CAF)	/	24.5(3)	23.5(2)	7.35(23)	−0.5045	0.0121(855)
CAF-1	−0.285(184)	39.94(5)	45.69(6)	11.42(8)	−0.6022	−0.08119(2402)
CAF-2	−0.047(237)	56.67(124)	54.10(33)	13.86(27)	−0.5914	−0.1177(57)
CAF-3	0.542(290)	26.42(16)	31.48(9)	10.58(19)	−0.4735	−0.03997(751)
CAF-4	2.163(325)	5.024(68)	3.262(13)	2.980(63)	−0.03924	−0.3210(1356)
CAF-5	3.722(227)	5.160(9)	5.584(2)	6.547(231)	0.06893	−0.07137(4156)

^a log *P* values of the conjugated acid for ancillary ligands were calculated using Advanced Chemistry Development (ACD/Labs) Software V8.14 for Solaris.

monocopper complex exists as a hydrated species, Cu(ASP)₂-(AL)₂(H₂O), in the aqueous phase (in ESI). This presumably increases the aqueous solubility and, thus, decreases its relative lipophilicity.

Within the Cu(II)–salsalate series, the order of log SR values for the Cu(II)–salsalate species with the same coordination chromophore reflects the order of log *P* values calculated for the ancillary ligands, which is also consistent

with the additive–constitutive character observed for organic congeners, the exception being that, although the log *P* value of 4-benzylpyridine is higher than that of 4-phenylpyridine, the log SR/log *P* value of **SAS-4** is smaller than that of **SAS-5**. This might be due to the uncertainty of calculated log *P* values of ancillary ligands. It is also worth noting that, although the log *P* values calculated for the ancillary ligands vary in a wide range (from −0.282 to 2.715), only the log

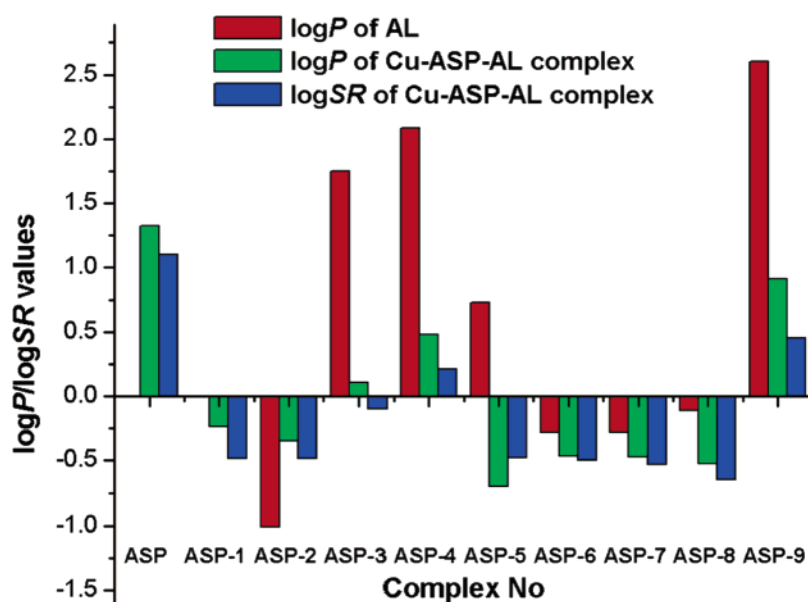


Figure 6. Calculated log P values for ancillary ligands (red); observed log P values for aspirin and Cu–ASP–AL complexes (green); observed log SR values for aspirin and Cu–ASP–AL complexes (blue).

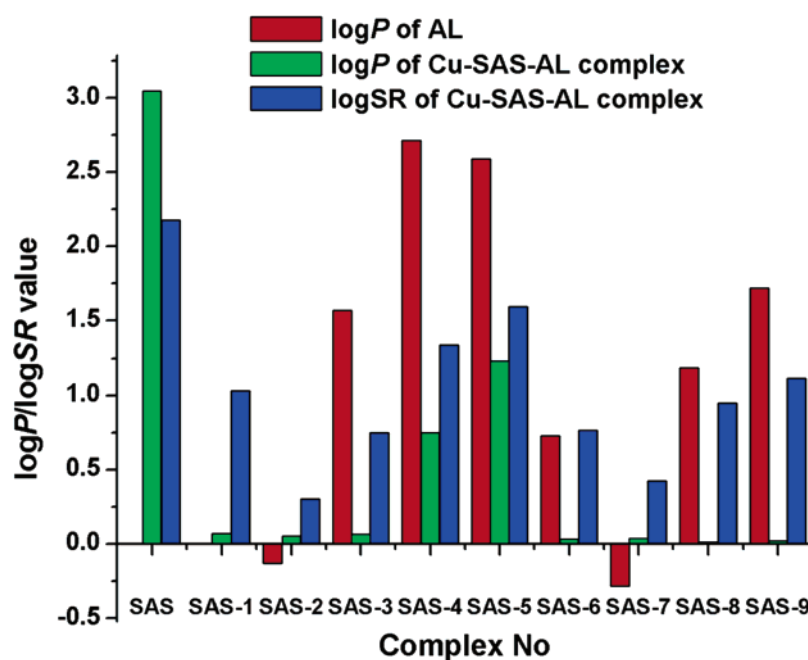


Figure 7. Calculated log P values for ancillary ligands (red); observed log P values for salsalate and Cu–SAS–AL complexes (green); observed log SR values for salsalate and Cu–SAS–AL complexes (blue).

P values of **SAS-4** and **SAS-5** were significantly increased via the introduction of aromatic ancillary ligands, Figure 7. This is attributed to size effects. Since the phenol groups in salsalate sterically shield the ancillary ligands, aqueous interactions will decrease, thus the log P values of Cu–salsalate–AL species with a small ancillary ligand do not change much. As exemplified in Figure 8, the ancillary ligands were shielded by salsalate phenol rings, and notably ancillary ligands in **SAS-2** and **SAS-5** are sandwiched between two phenol rings. So even if 4-benzylpyridine and

4-phenylpyridine are sterically shielded by salsalate phenol rings in some fashion, only the log P values of corresponding complexes **SAS-4** and **SAS-5** were still significantly increased because of the large molecular size of ancillary ligands.

Furthermore, there is also some degree of predictability in observed aqueous solubility based on the log P of the ancillary ligand. Generally with the increase of log P value of ancillary ligand, aqueous solubilities of Cu–API–AL congeners with the same coordination chromophore decrease, Tables 2 and 3.

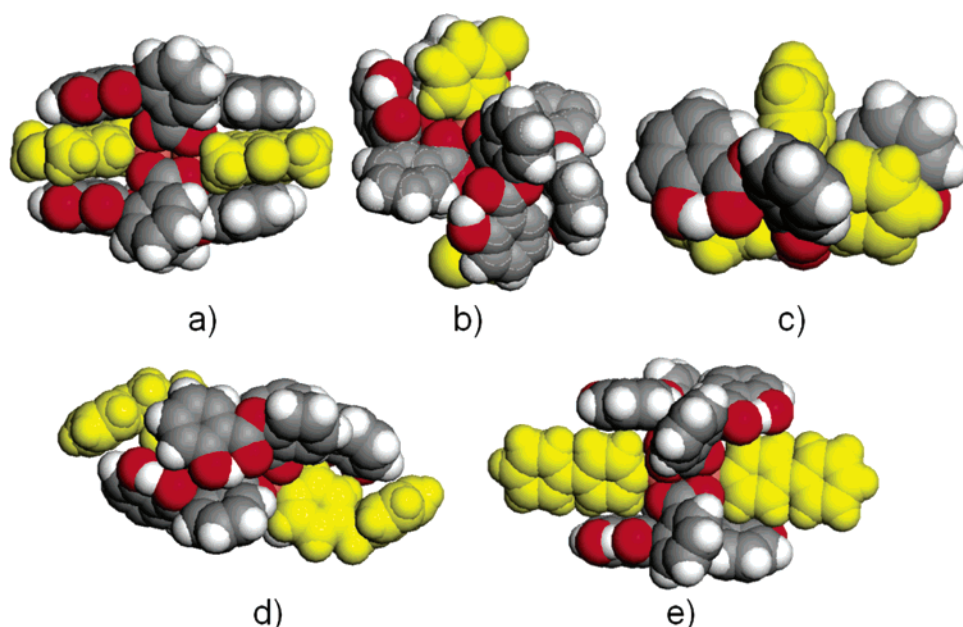


Figure 8. (a, b, c d, e) Single-crystal structure units of complexes **SAS-(2,3,6,4,5)** in CPK mode, respectively; ancillary ligands were labeled with yellow for clarity.

Mixed Anionic Ligand Complexes. Dinuclear Cu(II) paddle-wheel complexes with four identical carboxylates are ubiquitous, and only rare examples of mixed carboxylate dinuclear Cu(II) complexes are known so far.¹⁴ $\text{Cu}_2(\text{Ac})_2(\text{DMB})_2(\text{H}_2\text{O})_2$, $\text{Cu}_2(\text{DMB})_4(\text{H}_2\text{O})_2$ (HAc = acetic acid, $\text{H}(\text{DMB})$ = 2,6-dimethoxybenzoic acid), $\text{Cu}_2(\text{Ac})_2(\text{VA})_2(\text{H}_2\text{O})_2$, $\text{Cu}_2(\text{VA})_4(\text{H}_2\text{O})_2$ ($\text{H}(\text{VA})$ = vanillic acid) were prepared in water or wet alcohol. Then $\text{Cu}_2(\text{Ac})_4(\text{H}_2\text{O})_2$ (**MC-1**), $\text{Cu}_2(\text{Ac})_2(\text{DMB})_2(\text{H}_2\text{O})_2$ (**MC-2**), $\text{Cu}_2(\text{DMB})_4(\text{H}_2\text{O})_2$ (**MC-3**), $\text{Cu}_2(\text{Ac})_2(\text{VA})_2(\text{H}_2\text{O})_2$ (**MC-4**), and $\text{Cu}_2(\text{VA})_4(\text{H}_2\text{O})_2$ (**MC-5**) were investigated as *proof of principle* complexes, i.e., neither 2,6-dimethoxybenzoic acid nor vanillic acid is an API. Since the carboxylate ligand is “negatively” charged,

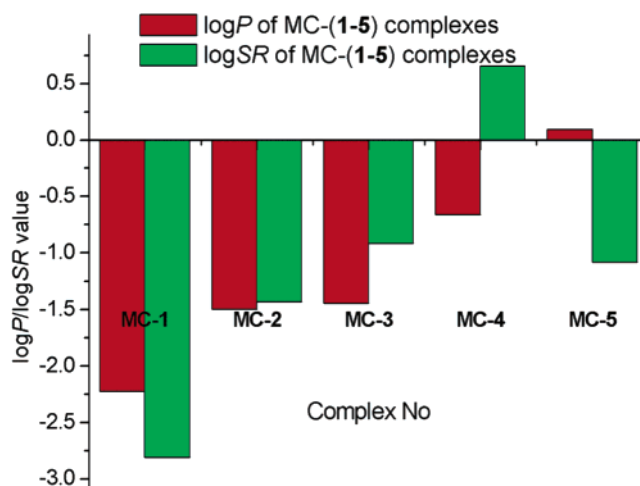


Figure 9. Observed log *P* and log SR values for complexes **MC-(1–5)**.

we can only compare the lipophilicity of their corresponding conjugated acid. The calculated log *P* values of acetic acid, 2,6-dimethoxybenzoic acid, and vanillic acid are -0.285 (184), 0.975 (256), and 1.334 (245), respectively.

As shown in Table 4 and Figure 9, the log *P*/log SR values for **MC-3** are significantly higher than those for **MC-1**, which indicates that **MC-3** is more lipophilic than **MC-1**. And the log *P*/log SR values for the mixed carboxylate complex, **MC-2**, are between the log *P*/log SR values for **MC-1** and **MC-3** (Table 4), which is also qualitatively consistent with the additive–constitutive character observed for organic congeners. A similar tendency has also been observed among **MC-1**, **-4**, and **-5**. The only exception is that the log SR value of **MC-5** is lower than the log SR value of **MC-4**, which is due to the low octanol solubility

- (14) Maspoeh, D.; Ruiz-molina, D.; Wurst, K.; Rovira, C.; Veciana, J. A very bulky carboxylic perchlorotriphenylmethyl radical as a novel ligand for transition metal complexes. A new spin frustrated metal system. *Chem. Commun.* **2002**, 2958–2959. Vives, G.; Mason, S. A.; Prince, P. D.; Junk, P. C.; Steed, J. W. Intramolecular versus Intermolecular Hydrogen Bonding of Coordinated Acetate to Organic Acids: A Neutron, X-ray, and Database Study. *Cryst. Growth Des.* **2003**, 3, 699–704. Strinnaerre, L.; Micera, G.; Piu, P.; Cariati, F.; Ciani, G. Synthesis, Spectral Properties, and Crystal and Molecular Structure of Tetrakis(μ -2,6-dimethoxybenzoato)diaquadicopper(II) and of Bis(μ -2,6-dimethoxybenzoato)bis(μ -acetato)diaquadicopper(II), a Case of a Dimeric Copper(II) Carboxylate Complex with Mixed Bridges. *Inorg. Chem.* **1985**, 24, 2297–2300. Banares, M. A.; Dauphin, L.; Lei, X.; Cen, W.; Shang, M.; Wolf, E. E.; Fehlner, T. P. Effect of Precursor Core Structure on the Hydrogenation of 1,3-Butadiene Catalyzed by Cluster-Derived Model Catalysts. *Chem. Mater.* **1995**, 7, 553–561. Kozlevcar, B.; Odlazek, D.; Golobic, A.; Pevec, A.; Strauch, P.; Segedin, P. Complexes with lignin model compound acid. Two different carboxylate ligands in the same dinuclear tetracarboxylate complex $[\text{Cu}_2(\text{C}_8\text{H}_7\text{O}_4)_2(\text{O}_2\text{CCH}_3)_2(\text{CH}_3\text{OH})_2]$. *Polyhedron* **2006**, 25, 1161–1166.

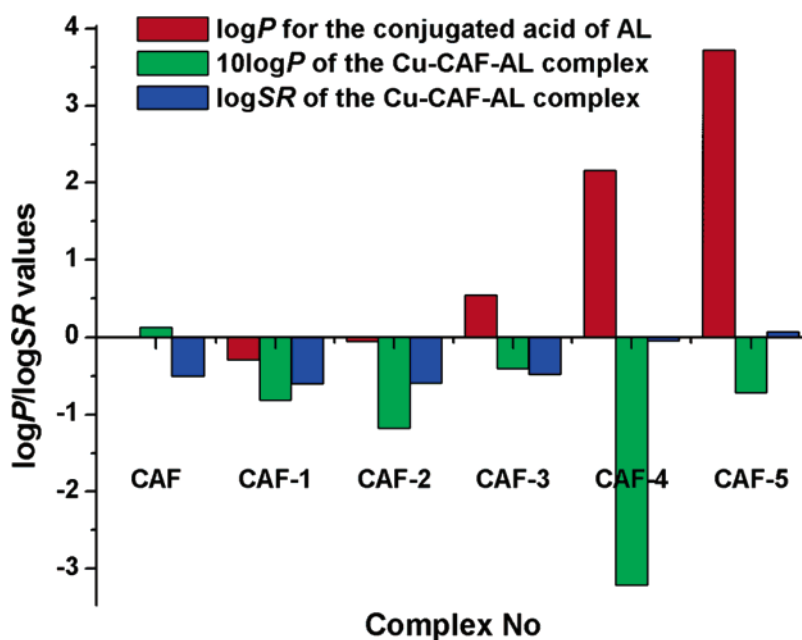


Figure 10. Calculated $\log P$ values for the conjugated acid of ancillary ligands (red); observed $\log P$ values for caffeine and Cu-CAF-AL complexes (green), the $\log P$ was multiplied by 10 on the graph for clarity; observed $\log SR$ values for caffeine and Cu-CAF-AL complexes (blue).

for **MC-5**, Table 4. Presumably the low S_{wo} value for **MC-5** resulted from the relatively high lattice energy. Particularly, the $\log P$ value for **MC-2** is slightly lower than the $\log P$ value for **MC-3**. This is due to the small size of acetate anion, which cannot effectively change the lipophilicity by ligand substitution.

Neutral API with Anionic AL. Caffeine (CAF) is one imidazole-type purine alkaloid with interesting pharmacological properties. Copper(II)-carboxylate-(imidazole-type AL) mixed-ligand species have also been found to have a variety of pharmacological effects such as anticancer,¹⁴ superoxide dismutase,¹⁵ and catecholase mimetic activities.¹⁶ Table 5 lists solubility, partition coefficient, and solubility ratio for each prepared copper(II)-carboxylate-caffeine complex. As mentioned above, since the carboxylate ligand is “negatively” charged, the calculated $\log P$ value for the corresponding conjugated acid was used as a quantitative parameter.

Within this series of compounds, the order of $\log SR$ values follows the order of $\log P$ values for the conjugated acid of the ancillary ligands, Figure 10. Complexes **CAF-(1–5)** fall into two categories based on the observed $\log P$

values. **CAF-(1–3)**: The $\log P$ values for complexes **CAF-(1–3)** are close to the $\log P$ value of caffeine. The $\log P$ for **CAF-3** is the highest among these three species because of the relatively higher $\log P$ value of dichloroacetic acid than acetic acid and monochloroacetic acid. **CAF-(4,5)**: The order of observed $\log P$ values also follows the order of $\log P$ values for the conjugated acid of the ancillary ligands. However, even if the $\log P$ values of 2-iodobenzoic acid and ibuprofen are higher than those of acetic acid/monochloroacetic acid/dichloroacetic acid, the $\log P$ values for **CAF-(4,5)** are lower than the $\log P$ values for **CAF-(1–3)**. Presumably this is due to the small size of the ancillary ligands in **CAF-(1–3)**, which also explains why the $\log P$ values for **CAF-(1–3)** are closer to caffeine’s $\log P$ value.

In addition, our electrospray mass spectrometry¹⁸ and DOSY¹⁹ NMR data suggested that the mixed-ligand Cu(II) species are stable in the aqueous phase (see details in ESI), which ensures the validity of data measured in this work.

- (15) Tamua, H.; Imai, H.; Kuwahara, J.; Sugura, Y. A new antitumor complex: bis(acetato)bis(imidazole)copper(II). *J. Am. Chem. Soc.* **1987**, *109*, 6870–6871.
- (16) Bhirud, R. G.; Srivastava, T. S. Superoxide dismutase activity of Cu(II)₂(aspirinate)₄ and its adducts with nitrogen and oxygen donors. *Inorg. Chim. Acta* **1990**, *173*, 121–125.
- (17) Abuhijleh, A. L.; Woods, C.; Bogas, E.; LeGuenniou, G. Synthesis, characterization and catecholase-mimetic activity of mononuclear copper(II) aspirinate complexes. *Inorg. Chim. Acta* **1992**, *195*, 67–71.

- (18) Jones, E. C.; Taylor, P. J.; McEwan, A. G.; Hanson, G. R. Spectroscopic Characterization of Copper(II) Binding to the Immunosuppressive Drug Mycophenolic Acid. *J. Am. Chem. Soc.* **2006**, *128*, 9378–9386.
- van den Brenk, A. L.; Byriel, K. A.; Fairlie, D. P.; Gahan, L. R.; Hanson, G. R.; Hawkins, C. J.; Jones, A.; Kennard, C. H. L.; Moubarak, B.; Murray, K. S. Crystal Structure, Electrospray Ionization Mass Spectrometry, Electron Paramagnetic Resonance, and Magnetic Susceptibility Study of [Cu₂(ascidH₂)(1,2-μ-CO₃)(H₂O)₂·2H₂O], the Bis(copper(II)) Complex of Asciadiacyclamide (ascidH₄), a Cyclic Peptide Isolated from the Ascidian *Lissoclinum patella*. *Inorg. Chem.* **1994**, *33*, 3549–3557.

Discussion

The introduction of ancillary ligands can form a homologous series of metal–drug complexes with variable lipophilicity and solubility. The solubility and lipophilicity of a drug are regarded as important *in vitro* ADMET parameters.²⁰ In particular, the relative potency of the drug is related to its lipophilicity by a certain mathematical representation.²¹ So the introduction of ancillary ligands may also be expected to modify the potency and efficacy of the parent metal–drug complexes.

In the current study, our data suggest that the formation of mixed-ligand coordination species can be developed as a complementary technique to pharmaceutical cocrystals for fine-tuning critical ADMET parameters without altering the parent drug compound via organic transformations. The most significant finding of this work is that we have demonstrated that there is some degree of predictability in the observed lipophilicity and solubilities based on the log *P* of the ancillary ligand. More specifically, additive–constitutive strategies to tune the lipophilicity of organic molecules can be qualitatively extended to metal–drug complexes. The nature of the chromophore, hydrogen bonds, and relative size of the ligands are also important factors that affect the lipophilicity of metal–drug complexes.

Indeed, “the use of metal ions in medicine is not new. What is new, [however], is the increasing purposeful design of metal-based therapeutics.”²² Our work is aimed toward developing a general and rational approach to the modification of metal–drug complexes. Some reported results have indicated that the efficacy of metal–drug complexes can be improved by the introduction of the proper ancillary ligand.²³ There are also other advantages of the introduction of ancillary ligand over altering the parent drug compound via organic transformations: easy preparation, integrity of API,

lower cost. One of the anticipated concerns regarding the use of metal-based coordination species may be the accumulation and toxicity of the metal. Since many transition metals are considered dietary micronutrients (i.e., Cr, Mn, Fe, Cu, Zn), the daily intake of certain transition metals under the Tolerable Upper Intake level is supposed to pose no risk of adverse health effects for almost all individuals in the general population.²⁴ For instance, copper complexes were reported for the treatment of chronic diseases;²⁵ some copper and zinc complexes have been used in clinical trials.²⁶ We have therefore initially targeted these metals in our studies. Clearly, the uptake of metal-containing complexes should be within the pharmaceutically beneficial ranges to avoid metal overload toxicity.²⁷ Furthermore, the specific materials presented in this work were prepared as *proof-of-principle* complexes; therefore toxicity is not specifically addressed in this study.

In conclusion, this work underscores the idea that complexes that incorporate transition metals coordinated to drug ligands and property-directing ancillary ligands offer a promising approach for the development of new or existing therapeutic embodiments. More generally, supramolecular synthesis—which includes metal complexes and cocrystals—is expected to be a valuable tool for fine-tuning critical physical properties, improving processability, and extending or widening intellectual property protection for a drug that

- (19) Morris, K. F.; Johnson, C. S. Diffusion-ordered two-dimensional nuclear magnetic resonance spectroscopy. *J. Am. Chem. Soc.* **1992**, *114*, 3139–3141. Morris, K. F.; Johnson, C. S. Resolution of discrete and continuous molecular size distributions by means of diffusion-ordered 2D NMR spectroscopy. *J. Am. Chem. Soc.* **1993**, *115*, 4291–4299. Allouche, L.; Marquis, A.; Lehn, J. Discrimination of Metallosupramolecular Architectures in Solution by Using Diffusion Ordered Spectroscopy (DOSY) Experiments: Double-Stranded Helicates of Different Lengths. *Chem. Eur. J.* **2006**, *12*, 7520–7525. Claridge, T. D. W. *High-Resolution Nmr Techniques in Organic Chemistry*; Elsevier: New York, 1999; pp 187–200.
- (20) Lipinski, C. A.; Lombardo, F.; Dominy, B. W.; Feeney, P. J. Experimental and computational approaches to estimate solubility and permeability in drug discovery and development settings. *Adv. Drug Delivery Rev.* **1997**, *23*, 3–25.
- (21) Hansch, C.; Steward, A. R.; Anderson, S. M.; Bentley, D. Parabolic dependence of drug action upon lipophilic character as revealed by a study of hypnotics. *J. Med. Chem.* **1968**, *11*, 1–11.
- (22) Thompson, K. H.; Orvig, C. Boon and Bane of Metal Ions in Medicine. *Science* **2003**, *300*, 936–939.
- (23) van Kralingen, C. G.; Reedijk, J.; Spek, A. L. Synthesis and characterization of antitumor-active platinum 2,2-dimethyl-1,3-diaminopropane compounds. Crystal and molecular structure of (malonato)(2,2-dimethyl-1,3-diaminopropane)platinum(II). *Inorg. Chem.* **1980**, *19*, 1481–1485.
- (24) Food & Nutrition Board Standing Committee on the Scientific Evaluation of Dietary Reference. *Dietary Reference Intakes: For Vitamin A, Vitamin K, Arsenic, Boron, Chromium, Copper, Iodine, Iron, Manganese, Molybdenum, Nickel, Silicon, Vanadium, and Zinc*; Natl Academy Press: Washington, DC, 2002; pp 7–8.
- (25) Sorenson, J. R. Copper complexes offer a physiological approach to treatment of chronic disease. *Prog. Med. Chem.* **1989**, *26*, 437–568.
- (26) Shackel, N. A.; Day, R. O.; Kellett, B.; Brooks, P. M. Copper-salicylate gel for pain relief in osteoarthritis: a randomised controlled trial. *Med. J. Aust.* **1997**, *167*, 134–136. Okada, A.; Takagi, Y.; Nezu, R.; Lee, S. Zinc in clinical surgery—a research review. *Jpn. J. Surg.* **1990**, *20*, 635–644.
- (27) Cameron, B. R.; Baird, I. R. Metals in Medicine: a review of the symposium. *J. Inorg. Biochem.* **2001**, *83*, 233–236. Barceloux, D. G. Copper. *Clin. Toxicol.* **1999**, *37*, 217–230.
- (28) Underhill, A. E.; Bury, A.; Odling, R. J.; Fleet, M. B.; Stevens, A.; Gomm, P. S. Metal complexes of antiinflammatory drugs. Part VII: Salsalate complex of copper(II). *J. Inorg. Biochem.* **1989**, *37*, 1–5.
- (29) Melnik, M. BINUCLEAR CAFFEINE ADDUCTS OF Cu(II) ACETATE AND Cu(II) CHLOROACETATES WITH UNUSUALLY HIGH ANTIFERROMAGNETIC INTERACTION. *J. Inorg. Nucl. Chem.* **1981**, *43*, 3035–3038.
- (30) Valach, F.; Tokarcik, M.; Maris, T.; Watkin, D. J.; Prout, C. K. Bond-valence approach to the copper–copper and copper–nitrogen bonding in binuclear copper(II) complexes: Structure of tetrakis(2-iodobenzoato)bis(caffeine)dycopper(II) at 210K. *J. Organomet. Chem.* **2001**, *622*, 166–171.
- (31) Latif Abuhijleh, A. Mononuclear and binuclear copper(II) complexes of the antiinflammatory drug ibuprofen: Synthesis, characterization, and catecholase-mimetic activity. *J. Inorg. Biochem.* **1994**, *55*, 255–262.

is in development. Inherent in our entitling this methodology *supramolecular medicinal chemistry* is the contention that this methodology deserves greater attention at the earlier stages of the development cycle, although it has demonstrated benefits in formulation as well. Current studies are investigating the additive—constitutive character of $\log P$ of the drug ligand to the solubility profile, and complex stability with respect to acidic environments. Moreover, we are directing our research toward therapeutic targets for which solubility issues are greater concerns and for which there is intuitively a greater tolerance for formulations containing transition metals, such as cancer and other chronic or life-threatening diseases.

Abbreviations Used

ADMET, absorption, distribution, metabolism, excretion, and toxicity; API, active pharmaceutical ingredient; AL,

ancillary ligand; QSAR, quantitative structure—activity relationships; ow, octanol-saturated water; wo, water-saturated octanol; SR, solubility ratio (S_{wo}/S_{ow}); ASP, aspirin and copper(II)—aspirinate complexes; SAS, salsalate and copper(II)—salsalate complexes; MC, mixed carboxylate copper(II) complexes; CAF, caffeine and copper(II) carboxylate—caffeine complexes.

Acknowledgment. This work has been supported in part by MRDA (Moldova)—CRDF (U.S.) award No. MRDA-008: BGP-III, MOC2-3063-CS-03.

Supporting Information Available: Crystallographic data, ESI-MS spectra, and DOSY spectrum for model complexes. This material is available free of charge via the Internet at <http://pubs.acs.org>.

MP070013K